
RELIABILITY-ADJUSTED PRIORITIZED EXPERIENCE REPLAY

Leonard S. Pleiss

Technical University Munich
Munich, 80331
leonard.pleiss@tum.de

Tobias Sutter

University St. Gallen
St. Gallen, 9000
tobias.sutter@unisg.ch

Maximilian Schiffer

Technical University Munich
Munich, 80331
schiffer@tum.de

ABSTRACT

Experience replay enables data-efficient learning from past experiences in online reinforcement learning agents. Traditionally, experiences were sampled uniformly from a replay buffer, regardless of differences in experience-specific learning potential. In an effort to sample more efficiently, researchers introduced Prioritized Experience Replay (PER). In this paper, we propose an extension to PER by introducing a novel measure of temporal difference error reliability. We theoretically show that the resulting transition selection algorithm, Reliability-adjusted Prioritized Experience Replay (ReaPER), enables more efficient learning than PER. We further present empirical results showing that ReaPER outperforms PER across various environment types, including the Atari-5 benchmark.

Keywords Deep Reinforcement Learning · Temporal Difference Learning · Experience Replay

1 Introduction

Reinforcement Learning (RL) agents improve by learning from past interactions with their environment. A common strategy to stabilize learning and improve sample efficiency is to store these interactions—called transitions—in a replay buffer and reuse them through experience replay to increase sample-efficiency. When using experience replay, the agent obtains mini-batches for training by sampling transitions from the replay buffer. Rather than sampling uniformly from this buffer, various prioritization schemes aim to select the most informative transitions, improving convergence speed and, ultimately, policy performance.

The most prominent sampling scheme that represents today’s state of the art is PER, introduced in Schaul et al. [2015]. PER samples transitions in proportion to their absolute Temporal Difference Error (TDE), which measures the distance between predicted and target Q-values. Accordingly, PER follows the rationale that transitions with higher absolute TDEs bear higher learning potential. While this rationale is intuitive, the TDE is a biased proxy as both the predicted and the target Q-value are approximations. Hence, prioritizing transition selection based on absolute TDEs can misdirect learning, potentially leading to degrading value estimates, if the target Q-value is itself inaccurate. Such inaccurate targets may dampen convergence or in the worst case deteriorate final policy performance.

To mitigate this bias, we propose ReaPER, an improved sampling scheme that adjusts the prioritization of transitions by accounting for the reliability of target Q-values. ReaPER maintains the strengths of PER while avoiding ineffective training on misleading updates caused by unreliable targets. If the agent has not yet learned to accurately assess future states, the target Q-value becomes unreliable, and, consequently, the TDE may become a poor proxy for sample prioritization.

This rationale becomes particularly intuitive in game environments such as Go, Chess, or Tic Tac Toe. Consider a player assessing the current board position: if they lack a reliable understanding of how the game might unfold, their evaluation of the current state’s value is likely inaccurate. As shown in Figure 1, states closer to terminal outcomes (i.e., near the end of the game) involve fewer remaining moves, making it easier for the agent to accurately estimate their values. Early-game states, in contrast, rely on longer and more uncertain rollouts. Thus, value estimates tend to be more reliable as one moves closer to the end of an episode. This observation implies a hierarchical dependency in the learning

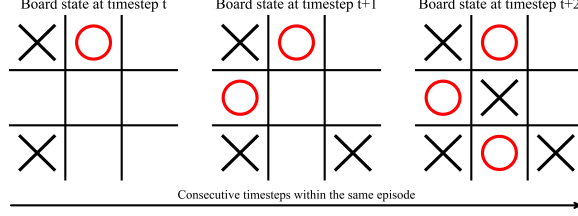


Figure 1: Subsequent states from a Tic Tac Toe game from the perspective of the agent placing circles. Board state $t + 2$ is terminal. States t and $t + 1$ are losing under optimal play. For an inexperienced player, recognizing that $t + 1$ is a losing state is generally easier than recognizing t as such. However, once $t + 1$ is understood as losing, identifying t as lost becomes more straightforward. In general, accurately assessing $t + 1$ is a prerequisite for reliably assessing t —especially when learning the game without explicit knowledge of rules or win conditions. As long as the agent’s assessment of $t + 1$ is flawed, its evaluation of t remains unreliable.

of transitions within a trajectory, wherein the accurate estimation of earlier state-action values is conditioned on the agent’s ability to infer and propagate information from later transitions. Consequently, we suggest that the reliability of target values—and by extension, of TDEs—should factor into experience replay prioritization.

State of the Art Experience replay has been an active field of research for decades. After its first conceptualization by Lin [1992], various extensions, analyses and refinements have been proposed (e.g., Andrychowicz et al. [2017], Zhang and Sutton [2017], Isele and Cosgun [2018], Rolnick et al. [2018], Rostami et al. [2019], Fedus et al. [2020], Lu et al. [2023]).

Central to our work is an active stream of research exploring optimized selection of experiences from the replay buffer. The most notable contribution in this stream so far was PER (Schaul et al. [2015]). In essence, PER proposes to use the absolute TDE as a sampling weight, which allows to select transitions with a high learning potential more frequently compared to a uniform sampling strategy. Various papers built upon the idea of using transition information as a transition selection criterion: Ramicic and Bonarini [2017] explored an entropy-based selection criterion. Gao et al. [2021] proposed using experience rewards for sample prioritization. Lee et al. [2018] proposed Episodic Backwards Update, a method of leveraging past experiences using recursive multi-step updates. Brittain et al. [2019] introduced Prioritized Sequence Experience Replay, which extends PER by propagating absolute TDEs backwards throughout the episode before using them as a sampling criterion. Zha et al. [2019] and Oh et al. [2021] proposed dynamic, learning-based transition selection mechanisms. Yet, the proposed approaches have not replaced PER as the state-of-the-art, owing to its effectiveness, implementation simplicity, and low computational cost.

Contribution We propose ReaPER, a novel experience replay sampling scheme that improves upon PER by reducing the influence of unreliable TD targets, ultimately leading to more stable learning and better policy performance. Specifically, our contribution is threefold: first, we propose the concept of target Q-value and TDE reliability and introduce a reliability score based on the absolute TDEs in subsequent states of the same trajectory. Second, we present formal results proving the effectiveness of the reliability-adjusted absolute TDE as a transition selection criterion. Third, we leverage the theoretical insights and the novel reliability score to propose ReaPER, a sampling scheme facilitating more effective experience replay. The proposed method is algorithm-agnostic and can be used within any off-policy RL algorithm.

To substantiate our theoretical findings, we perform numerical experiments comparing ReaPER to PER across various traditional RL environments, namely CARTPOLE, ACROBOT, LUNARLANDER and the ATARI-5 benchmark (Aitchison et al. [2022]). We show that ReaPER consistently outperforms PER. Specifically, in environments of lower complexity like CARTPOLE, ACROBOT and LUNARLANDER, ReaPER reaches the maximum score on average between 21.35% and 29.49% faster. In environments of higher complexity, exemplified by the ATARI-5 benchmark, ReaPER on average achieves a 30.18% ($SD = 28.50$) higher peak performance.

2 Problem statement

We consider a standard Markov decision process (MDP) as usually studied in an RL setting [Sutton and Barto, 1998]. We characterize this MDP as a tuple $(\mathcal{S}, \mathcal{A}, P, r, \gamma, p)$, where \mathcal{S} is a finite state space, \mathcal{A} is a finite action space, $P : \mathcal{S} \times \mathcal{A} \rightarrow \Delta(\mathcal{S})$ is a stochastic kernel, $r : \mathcal{S} \times \mathcal{A} \rightarrow \mathbb{R}$ is a reward function, $\gamma \in (0, 1)$ is a discount factor, and

$p \in \Delta(\mathcal{S})$ denotes a probability mass function denoting the distribution of the initial state, $S_1 \sim p$. At time step t , the system is in state $S_t = s \in \mathcal{S}$. We denote by S_t and A_t the random variables representing the state and action at time t , and by $s \in \mathcal{S}$ and $a \in \mathcal{A}$ their respective realizations. If an agent takes action $A_t = a \in \mathcal{A}$, it receives a corresponding reward $r(s, a)$, and the system transitions to the next state $S_{t+1} \sim P(\cdot | s, a)$. We define the random reward at time t as $R_t = r(S_t, A_t)$. The agent selects actions based on a policy $\pi : \mathcal{S} \rightarrow \mathcal{A}$ via $A_t = \pi(S_t)$.

Let $\mathbb{P}_p^\pi(\cdot) = \text{Prob}(\cdot | \pi, S_1 \sim p)$ denote the probability of an event when following a policy π , starting from an initial state $S_1 \sim p$, and let $\mathbb{E}_p^\pi[\cdot]$ denote the corresponding expectation operator. We consider problems with finite episodes, where n expresses the number of transitions within the episode. Let G_t denote the discounted return at time t , $G_t = \sum_{i=t}^n \gamma^{i-t} R_i$. We define the Q-function (or action-value function) for a policy π as

$$Q^\pi(s, a) = \mathbb{E}_p^\pi [G_t | S_t = s, A_t = a] = \mathbb{E}_p^\pi \left[\sum_{i=t}^n \gamma^{i-t} R_i | S_t = s, A_t = a \right]. \quad (1)$$

The ultimate goal of RL is to learn a policy that maximizes the Q-function, leading to $Q^*(s, a) = \max_\pi Q^\pi(s, a)$. The policy is gradually improved by repeatedly interacting with the environment and learning from previously experienced transitions. A transition C_t is a 5-tuple, $C_t = (S_t, A_t, R_t, S_{t+1}, d_t)$, where d_t is a binary episode termination indicator, $d_t = \mathbb{1}_{t=n}$. One popular approach to learn Q^* is via Watkins' Q-learning (Watkins [1989], Watkins and Dayan [1992]), where Q-values are gradually updated via

$$Q(S_t, A_t) \leftarrow Q(S_t, A_t) + \eta \cdot \delta_t \quad (2)$$

in which $\eta \in (0, 1]$ is the learning rate and δ_t the TDE, $\delta_t = Q_{\text{target}}(S_t) - Q(S_t, A_t)$ with $Q_{\text{target}}(S_t) = R_{t+1} + (1 - d_{t+1}) \cdot \gamma \cdot \max_a Q(S_{t+1}, a)$. For brevity of notation, we refer to the absolute TDE as $\delta_t^+ = |\delta_t|$.

In practical RL applications, experience replay is commonly employed to stabilize and accelerate learning. Transitions collected through agent-environment interaction are stored in a finite buffer $\mathcal{H} = \{C_t\}_{t=1}^N$, from which mini-batches $\mathcal{X} \subset \mathcal{H}$ of fixed size $|\mathcal{X}| = k$ are sampled to update the Q-function. The sampling distribution over the buffer, denoted by $\mu \in \Delta(\mathcal{H})$, determines the likelihood $\mu(C_t)$ of selecting transition $C_t \in \mathcal{H}$ when constructing \mathcal{X} . In uniform experience replay, μ is the uniform distribution, whereas in PER (Schaul et al. [2015]), transitions are sampled according to scalar priority values, derived from the absolute TDE δ_t^+ .

Empirical evidence suggests that the effectiveness of the learning process is sensitive to the choice of μ , i.e., sampling transitions with high learning potential can improve convergence speed and final performance. However, designing an optimal or near-optimal sampling distribution remains an open problem. With this work, we aim to contribute to closing this gap by defining and efficiently approximating a sampling distribution μ^* that maximizes learning progress using experience replay.

3 Methodology

In the following, we provide the methodological foundation for ReaPER. We first introduce a reliability score for absolute TDEs, which we use to derive a TDE-based reliability-adjusted transition sampling method. We then provide theoretical evidence for its efficacy.

3.1 Reliability score

In bootstrapped value estimation, as in Q-learning, the target value

$$Q_{\text{target}}(S_t) = R_{t+1} + \gamma \cdot (1 - d_{t+1}) \cdot \max_a Q(S_{t+1}, a) \quad (3)$$

relies on the current estimate of future values. Consequently, the quality of an update to $Q(S_t, A_t)$ depends not only on the magnitude of the absolute TDE δ_t^+ , but also on the reliability of the target value $Q_{\text{target}}(S_t)$.

We define the reliability of a target Q-value as a measure of how well it approximates the true future return from a given state-action pair. Intuitively, a target value is reliable if it decreases the distance between $Q^*(S_t, A_t)$ and $Q(S_t, A_t)$. Conversely, a target is unreliable if training on it increases the distance between $Q^*(S_t, A_t)$ and $Q(S_t, A_t)$.

To motivate this concept and formalize its operational consequences, we consider a single episode consisting of transitions (C_1, \dots, C_n) , from initial state S_1 to terminal state S_{n+1} . We highlight three key observations that explain how reliability varies along the trajectory and how it can be used to improve sampling:

Observation 3.1 (Unreliable targets can degrade learning). $Q_{\text{target}}(S_t)$ depends on the estimate $Q(S_{t+1}, \cdot)$ for $t \in \{1, \dots, n-1\}$, which may be inaccurate. If an update is based on a poor target value, the resulting $Q(S_t, A_t)$ may diverge from $Q^*(S_t, A_t)$, thereby degrading the estimate.

Observation 3.2 (Terminal transitions induce reliable updates). For terminal transitions, the target is given directly by the environment, i.e., $Q_{\text{target}}(S_n) = R_n$. This target is exact, implying that the corresponding TDE accurately reflects the deviation from the ground truth Q -value. Thus, updates based on terminal transitions are guaranteed to shift $Q(S_n, A_n)$ towards $Q^*(S_n, A_n)$ if $\delta_n^+ > 0$.

Observation 3.3 (Reliability propagates backward). An accurate update to $Q(S_t, A_t)$ improves the accuracy of $Q_{\text{target}}(S_{t-1})$ and earlier targets, which recursively depend on it. Therefore, updating transitions near the end of the episode helps improving the reliability of Q_{target} for earlier transitions.

These observations highlight a temporal hierarchy in transition learning: *Learning later transitions before learning earlier transitions appears advantageous*. On the one hand, later targets rely on fewer estimated quantities and are therefore more reliable. On the other hand, learning later transitions positively impacts the target reliability for earlier transitions. Furthermore, a high TDE indicates a misunderstanding of game dynamics for a given transition, thus rendering the value estimation in predecessor transitions—which rely on the understanding of the value dynamics in the subsequent rollout—less reliable. We therefore aim to resolve TDEs back-to-front. This motivates defining the reliability of $Q_{\text{target}}(S_t)$ inversely related to the sum of future absolute TDEs,

$$\mathcal{R}_t = 1 - \frac{\sum_{i=t+1}^n \delta_i^+}{\sum_{i=1}^n \delta_i^+}. \quad (4)$$

Using this definition, we propose the *reliability-adjusted TDE*

$$\Psi_t = \mathcal{R}_t \cdot \delta_t^+, \quad (5)$$

as a sampling criterion for selecting transitions during experience replay. High values of Ψ_t correspond to transitions that promise large updates and have reliable target values. Sampling weights p can be obtained by normalizing the sampling criterion with the sum of Ψ over all transitions.

3.2 Formal analysis

We consider a set of transitions that constitutes a single complete trajectory of length n , $\mathcal{D} = \{C_t\}_{t=1}^n$, where $C_t = (S_t, A_t, R_t, S_{t+1}, d_t)$.

Updates are based on the TDE $\delta_t = Q(S_t, A_t) - Q_{\text{target}}(S_t)$, using the standard bootstrapped target

$$Q_{\text{target}}(S_t) = R_t + \gamma(1 - d_t) \max_a Q(S_{t+1}, a). \quad (6)$$

Convergence A critical factor to ensure convergence in Q-learning is the alignment between the TDE and the true value estimation error $Q(S_t, A_t) - Q^*(S_t, A_t)$. When the bootstrapped target is biased, meaning $Q_{\text{target}}(S_t) \neq Q^*(S_t, A_t)$, the update direction may become misaligned, potentially worsening the value estimate.

We defer the formal misalignment analysis to Lemma B.1 and Lemma B.2 in Appendix B.1. In essence, the expected change in squared true value estimation error due to an update of the value function approximator under a sampling strategy μ can be decomposed into three components, the TDE variance, the true squared error, and the bias-error interaction

$$\mathbb{E}_\mu[\Delta|Q(S_t, A_t) - Q^*(S_t, A_t)|^2] = \underbrace{\eta^2 \sum_{t=1}^n \mu_t \mathbb{E}[\delta_t^2]}_{\text{TDE variance}} - \underbrace{2\eta \sum_{t=1}^n \mu_t \mathbb{E}[e_t^2]}_{\text{True squared error}} + \underbrace{2\eta \sum_{t=1}^n \mu_t \mathbb{E}[e_t \varepsilon_t]}_{\text{Bias-error-interaction}}, \quad (7)$$

where e_t denotes the true value error, and ε_t denotes the target bias,

$$e_t = Q(S_t, A_t) - Q^*(S_t, A_t), \quad \varepsilon_t = Q_{\text{target}}(S_t) - Q^*(S_t, A_t). \quad (8)$$

By focusing on large TDEs, PER aims to sample transitions with higher true squared error more frequently, thus resolving errors faster and improving efficiency over uniform sampling. In the following, we show that our ReaPER sampling scheme additionally controls the target bias, thereby minimizing the bias-error interaction, while also preserving the advantages of PER. This allows ReaPER to increase sampling-efficiency over PER. To do so, we base the following formal analyses on a key assumption relating target bias to absolute downstream TDEs.

Assumption 3.4 (Target Bias via Downstream TDEs). *Along an optimal trajectory, the target bias ε_t for each transition C_t satisfies*

$$|\varepsilon_t| \leq \lambda \sum_{i=t+1}^n \delta_i^+, \quad (9)$$

This assumption formalizes the intuition that bootstrapped targets primarily inherit bias from inaccuracies in future predictions. It reflects standard TD-learning dynamics under sufficient exploration and function approximation stability. In a nutshell, it captures the intuition that target bias predominantly arises from unresolved downstream TDEs, reflecting a local perspective on TD-learning dynamics. Unlike classical convergence proofs that require global exploration and decaying learning rates, our assumption focuses on bounding the bias along observed trajectories during finite-sample learning, making it more applicable to practical deep RL. We refer the interested reader to Appendix B.2 for a detailed discussion.

Under Assumption 3.4, the reliability score \mathcal{R}_t —representing the fraction of downstream TDE within a given trajectory—bounds the normalized target bias. This is captured in the following lemma.

Lemma 3.5 (Reliability Bounds Target Bias). *Under Assumption 3.4,*

$$|\varepsilon_t| \leq \lambda(1 - \mathcal{R}_t) \sum_{i=1}^n \delta_i^+. \quad (10)$$

For the proof of Lemma 3.5, we refer to Appendix B.3. Lemma 3.5 expresses that transitions with higher reliability scores exhibit lower target bias and thus yield more trustworthy TDEs. This finding motivates selecting training transitions not just by TDE magnitude, but by a combination of TDE magnitude and reliability — as implemented in ReaPER.

Building on the established relationship between reliability and target bias, we derive the following convergence hierarchy.

Proposition 3.6 (Convergence Hierarchy of Sampling Strategies). *Under Assumption 3.4 and given a fixed learning rate η , ReaPER ($\mu_t \propto \mathcal{R}_t \delta_t^+$) yields lower expected Q -value error than standard PER ($\mu_t \propto \delta_t^+$), which in turn outperforms uniform sampling,*

$$\mathbb{E}[\|Q_T^{(\text{Uniform})} - Q^*\|^2] \geq \mathbb{E}[\|Q_T^{(\text{PER})} - Q^*\|^2] \geq \mathbb{E}[\|Q_T^{(\text{ReaPER})} - Q^*\|^2], \quad (11)$$

where \mathbb{E} denotes the expectation across training runs.

The corresponding proof, detailed in Appendix B.4, formally compares the expected error decrease terms under different sampling distributions, using Lemma 3.5 to bound the bias-error-interaction. While we limit Proposition 3.6 to optimal policies for brevity of notation, we can straightforwardly extend it to suboptimal policies.

Remark 3.7 (Extension to suboptimal policies). *If the agent follows a fixed but suboptimal policy, Assumption 3.4 can be relaxed to include an additive policy-induced bias term $\zeta \geq 0$, yielding*

$$|\varepsilon_t| \leq \lambda \sum_{i=t+1}^n \delta_i^+ + \zeta. \quad (12)$$

In this case, ReaPER still improves sampling efficiency in expectation, although the achievable Q -value accuracy is lower-bounded by the policy suboptimality ζ . For further details, we refer the interested reader to Appendix B.5.

Together, these results provide the theoretical foundation for ReaPER’s design: By prioritizing transitions with high absolute TDE and high reliability, ReaPER selects relevant transitions while improving alignment with the true value error, leading to faster and more stable learning.

Variance reduction In the following, we show that the proposed sampling scheme, based on reliability-adjusted TDEs reduces the variance of the Q -function updates. As a first step towards this result, we analyze the theoretically optimal distribution to sample from in order to minimize the variance of the Q -function update step. Recall that Q -values are updated according to (2), where the TDE corresponding to a transition C_t from the finite replay buffer \mathcal{H} reads $\delta_t = Q_{\text{target}}(S_t) - Q(S_t, A_t)$.

We assume a fixed episode and treat the current Q -values as constants, focusing on analyzing the update variance induced by the sampling distribution μ over \mathcal{H} . The update variance can then be expressed as

$$\sum_{t=1}^N \mu_t \text{Var}[\delta_t] = \sum_{t=1}^N \mu_t \text{Var}[Q_{\text{target}}(S_t)] = \sum_{t=1}^N \mu_t \sigma_t^2, \quad (13)$$

where the first equality follows from the definition of the TDE and the assumption that the current Q -values are constant. The second equality simply defines $\sigma_i^2 := \text{Var}[Q_{\text{target}}(S_i)]$ as the variance of the bootstrapped target for brevity.

Proposition 3.8 (Variance reduction via reliability-aware sampling). *The distribution μ^* minimizing the update variance (13) is given by*

$$\mu_t^* \propto \frac{\delta_t^+}{\sigma_t^2} \text{ for all } t \in \{1, \dots, N\} \quad (14)$$

For the proof of Proposition 3.8, we refer to Appendix B.6.

As a direct consequence of Proposition 3.8, we find that our proposed ReaPER sampling scheme is variance reducing if the reliability \mathcal{R} is proportional to the inverse variance of the bootstrapped target.

As the true target Q^* remains constant, a significant proportion of variance across runs for a given state can be attributed to the target bias. As such, there exists a direct relationship between ε and σ^2 . Hence, under Assumption 3.4, it seems natural to assume $\mathcal{R} \propto \frac{1}{\sigma^2}$. Thus, ReaPER constitutes a reasonable proxy for the optimal inverse-variance weighted sampling strategy.

To provide further intuition for our formal results, we have conducted a supplementary simulation-driven analysis showing that ReaPER achieves optimal transition selection in a stylized setting, which we detail in Appendix C.

4 Reliability-adjusted Prioritized Experience Replay

We have thus far introduced the reliability-adjusted TDE and theoretically proven its effectiveness as a transition selection criterion. In the following, we propose ReaPER, the sampling algorithm built around the reliability-adjusted TDE. We give a distilled overview of the resulting sampling scheme in Algorithm 1. At its core, we create mini-batches by sampling from the buffer with Ψ as the sampling weight. Specifically, at each training step $\tau \in \{1, \dots, T\}$, for every transition within the buffer, that is, C_t for all $t \in \{1, \dots, N\}$, we update TDE reliabilities \mathcal{R}_t and compute the reliability-adjusted transition selection criterion Ψ_t (Algorithm 1, Line 5ff.). Based on this transition selection criterion, we sample k transitions from the buffer \mathcal{H} to create the next mini-batch \mathcal{X} (Algorithm 1, Line 9ff.).

For the full algorithm and an extended explanation on how to embed it into an off-policy RL algorithm, we refer to Appendix A.

Algorithm 1: Sampling transitions and updating the value function using ReaPER

Input: absolute TDEs δ^+ , episode vector ϕ , current episode Φ , batch size k , exponents α, ω and β , replay buffer \mathcal{H} of size N , policy weights θ , maximum priority $p_{\max} = 1$, budget T

```

1 for  $\tau \in \{1, \dots, T\}$  do
2   Initialize accumulated weight change  $\Delta = 0$  and empty batch  $\mathcal{X} = \mathbf{0}^{(k)}$ ;
3   Add novel transitions to the buffer with maximum priority  $p_{\max}$  and set  $\phi_t = \Phi$ ;
4   Compute maximum episodic sum of absolute TDEs,  $F \leftarrow \max_{t \in \{1, \dots, N\}} \left( \sum_{i=1}^N \delta_i^+ \cdot \mathbb{1}_{\phi_t = \phi_i} \right)$ ;
5   for  $t \in \{1, \dots, N\}$  do                                     // Updating transition weights
6     Compute TDE reliabilities as in Formula 16;
7     Compute transition selection criterion  $\Psi_t \leftarrow \mathcal{R}_t^\omega \cdot \delta_t^{+\alpha}$ ;
8     Compute transition priorities  $p_t \leftarrow \frac{\Psi_t}{\sum_{i=1}^N \Psi_i}$ ;
9   for  $m \in \{1, \dots, k\}$  do                                     // Sampling transitions
10    Sample a transition  $C_j$  from  $\mathcal{H}$  to add to batch  $\mathcal{X}$  such that  $\mathbb{P}(C_t = \mathcal{X}_m) = p_t$  for all  $t \in \{1, \dots, N\}$ ;
11    Compute importance-sampling weight  $w_j \leftarrow \frac{(N \cdot p_j)^{-\beta}}{\max_t w_t}$  for all  $t \in \{1, \dots, N\}$ ;
12    Update  $\delta_j^+$  and accumulate weight-change  $\Delta \leftarrow \Delta + w_j \cdot \delta_j \cdot \nabla_\theta Q(S_j, A_j)$ ;
13  Update weights  $\theta \leftarrow \theta + \eta \cdot \Delta$ ;
14  Update maximum priority  $p_{\max} = \max(p_{\max}, \max(p))$ ;
```

Starting from the naive implementation of ReaPER, we require four technical refinements to obtain a functional and efficient sampling algorithm.

I. Priority updates. To consistently maintain an updated sampling weight Ψ , we track the TDEs and reliabilities of stored transitions throughout the training. As it is computationally intractable to re-calculate all TDEs on every model

update, we implement a leaner update rule: As in PER, we assign transitions maximum priority when they are added to the buffer. Moreover, we assign the TDE of transition C_t every time C_t is used to update the Q-function. We assign the reliability of transition C_t every time C_t is used to update the Q-function, or if any other transition from the same episode is used to update the Q-function, as it leads to a change in the sum of TDEs and possibly the subsequent TDEs. We update the priority Ψ when TDE or reliability are updated.

II. *Priority regularization.* As the TDE of a given transition may change by updating the model even without training on this transition, TDEs—and, in consequence, reliabilities—are not guaranteed to be up-to-date. Thus, similar to Schaul et al. [2015], we introduce regularization exponents $\alpha \in (0, 1]$ and $\omega \in (0, 1]$ to dampen the impact of extremely high or low TDEs or reliabilities,

$$\Psi_t = \mathcal{R}_t^\omega \cdot \delta_t^{+\alpha}. \quad (15)$$

III. *Reliabilities for ongoing episodes.* As the sum of TDE throughout an episode is undefined as long as the episode is not terminated, so is the reliability. In these cases, we use the maximum sum of TDEs of any episode within the buffer to obtain a conservative reliability estimate.

For this, we introduce ϕ , a vector of length N , where ϕ_t denotes the t -th position in ϕ , which contains a scalar counter of the trajectory during which transition C_t was observed. As such, ϕ functions as a positional encoding of transitions within the buffer. Specifically, it is used to identify all transitions that belong to the same trajectory. This positional encoding allows us to calculate conservative reliability estimates for a multi-episodic buffer.

We then define \mathcal{R}_t as

$$\mathcal{R}_t = \begin{cases} 1 - \left(\frac{\sum_{i=t+1}^n \delta_i^+}{\sum_{i=1}^n \delta_i^+} \right) & \text{for transitions of terminated episodes} \\ 1 - \left(\frac{F - \sum_{i=1}^t \delta_i^+}{F} \right) & \text{for transitions of ongoing episodes} \end{cases} \quad (16)$$

where

$$F = \max_{t \in \{1, \dots, N\}} \left(\sum_{i=1}^N \delta_i^+ \cdot \mathbb{1}_{\phi_t = \phi_i} \right) \quad (17)$$

VI) *Weighted importance sampling.* Finally, just as every other non-uniform sampling method, ReaPER violates the i.i.d. assumption. Thus, it introduces bias into the learning process, which can be harmful when used in conjunction with state-of-the-art RL algorithms. Similar to Schaul et al. [2015], we use weighted importance sampling (Mahmood et al. [2014]) to mitigate this bias. When using importance sampling, each transition C_t is assigned a weight w_t , such that

$$w_t = \left(\frac{1}{N} \cdot \frac{1}{p_t} \right)^\beta = \left(\frac{1}{N} \cdot \frac{\sum_{i=1}^N \Psi_i}{\Psi_t} \right)^\beta. \quad (18)$$

We use this weight to scale the loss and perform Q-learning updates using $\delta_t \cdot w_t$ instead of δ_t .

5 Numerical study

We evaluated ReaPER against PER across environments of varying complexity. For environments lower complexity, we used CARTPOLE, ACROBOT and LUNARLANDER. For environments of higher complexity, we used the ATARI-5 benchmark. Following prior work, we use ATARI-5 as a computationally efficient yet representative benchmark, ensuring relevance to broader Atari-57 evaluations without incurring prohibitive computational overhead [Aitchison et al., 2022]. Across conditions, we used the same Double Deep Q-Network (DDQN) agent, neural architecture, and model hyperparameters for all experiments. We controlled for all sources of randomness using fixed seeds and compared algorithms using identical seeds per trial. Thus, the only variation between conditions stemmed from the experience replay algorithm. Full experimental details and hyperparameters are provided in Appendix D.

Lower complexity environments Lower complexity environments usually require less training time, hence enabling more runs and allowing for a more reliable performance comparison. Thus, for each low complexity environment, we compared the performance between PER and ReaPER across 20 training runs. ReaPER outperformed PER across all environments. In the ACROBOT environment, both PER and ReaPER always achieved the maximum score of

−100. PER on average required 18,500 ($SD = 2,355.84$) training steps, ReaPER required 14,550 ($SD = 3,528.10$), decreasing the number of required learning steps by 21.35%. In the CARTPOLE environment, both PER and ReaPER always achieved the maximum score of 475. PER on average required 20,650 ($SD = 6,047.93$) training steps, ReaPER required 15,850 ($SD = 7,601.15$), decreasing the number of required learning time by 23.24%. In the LUNARLANDER environment, PER achieved the maximum score of 200 in 80% of training runs. ReaPER achieved the maximum score in 95% of training runs. PER on average required 54,600 ($SD = 30,775.64$) training steps, ReaPER required 38,500 ($SD = 24,270.35$), decreasing the number of required training steps by 29.49%, remarkably while simultaneously increasing the number of runs reaching a maximum score.

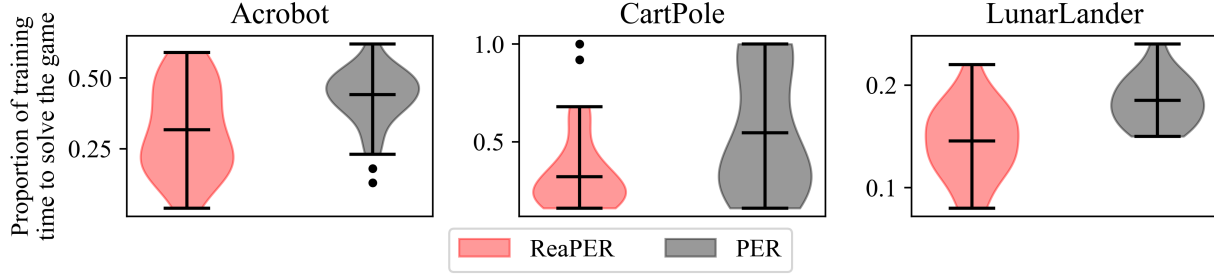


Figure 2: Proportion of training steps required by PER and ReaPER to reach a pre-defined score thresholds given in Towers et al. [2024] across 20 runs in three traditional RL environments. Outliers (displayed as points) were identified using Tukey’s method (Tukey [1977], $k = 1.5$).

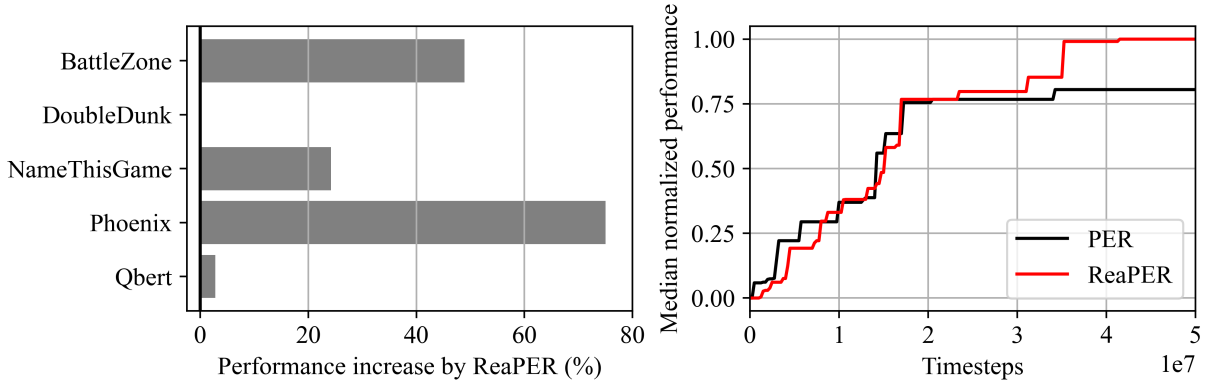


Figure 3: Left: Peak score increase of ReaPER over PER. Right: Median of the normalized cumulative sum of scores across the Atari-5 benchmark. The normalized score at timestep t is calculated by dividing the difference between the current score and the random score by the difference between the maximum score in this game across all sampling strategies and the random score.

Higher complexity environments For higher complexity environments, the ATARI-5 benchmark was used. The ATARI-5 benchmark is the most representative 5-game subset of the Atari-57 benchmark, which produces 57-game median score estimates within 10% of their true values [Aitchison et al., 2022]. ReaPER outperformed PER in four out of five games, and matched performance in one. Across all games, ReaPER achieved a 30.18% higher mean ($SD = 28.50$) and a 24.20% higher median peak score. These results underline ReaPER’s robustness across heterogeneous game dynamics and its ability to scale to challenging, high-dimensional domains. Detailed per-game curves are provided in Appendix E (Figure 6).

Discussion ReaPER consistently outperforms PER across all considered environments, indicating a substantial methodological advance. Notably, ReaPER did so with minimal hyperparameter tuning, suggesting that our reported results are a conservative estimate of ReaPER’s potential. We expect further gains through more extensive tuning of key hyperparameters, including regularization exponents α and ω , importance sampling exponent β and learning rate η .

A limitation of ReaPER is its reliance on terminal states, which are a pre-requisite for calculating meaningful TDE reliabilities. Further, ReaPER tracks the episodic cumulative sums of TDEs to calculate the reliability score, which causes computational overhead when TDEs are updated. Using a naive implementation, this overhead is non-negligible

at $O(N)$. However, it can be reduced to $O(n - t)$ by only re-calculating the episodic cumulative sums for transitions on their update or the update of a preceding transition within the same episode.

Finally, ReaPER targets unreliabilities in target Q-values, which can arise from two sources, initialization and erroneous generalization. While the former affects both tabular and deep learning settings and diminishes as the agent gains experience, the latter only affects deep learning settings but persists throughout training, where updates to one state-action pair may inadvertently alter unrelated estimates. Thus, controlling for target reliability is particularly critical in deep RL, where generalization-induced unreliabilities are ubiquitous.

6 Conclusion

We introduced ReaPER, a reliability-adjusted experience replay method that mitigates the detrimental effects of unreliable targets in off-policy deep reinforcement learning. By formally linking target bias to downstream temporal difference errors, we proposed a principled reliability score that enables more efficient and stable sampling. Our theoretical analysis shows that ReaPER improves both convergence speed and variance reduction over standard PER, and our empirical results confirm its effectiveness across diverse benchmarks.

Beyond its immediate practical gains, ReaPER highlights the importance of accounting for target reliability in experience replay, particularly in deep RL settings where function approximation errors and generalization artifacts are prevalent. We believe our work opens new avenues for incorporating uncertainty and reliability estimates into replay buffers, and future research may explore adaptive reliability estimation, extensions to actor-critic methods, and integration with representation learning.

References

- Tom Schaul, John Quan, Ioannis Antonoglou, and David Silver. Prioritized Experience Replay. 2015. doi: 10.48550/ARXIV.1511.05952. URL <https://arxiv.org/abs/1511.05952>.
- Long-Ji Lin. Self-improving reactive agents based on reinforcement learning, planning and teaching. *Machine Learning*, 8(3-4):293–321, May 1992. ISSN 0885-6125, 1573-0565. doi: 10.1007/BF00992699. URL <http://link.springer.com/10.1007/BF00992699>.
- Marcin Andrychowicz, Filip Wolski, Alex Ray, Jonas Schneider, Rachel Fong, Peter Welinder, Bob McGrew, Josh Tobin, Pieter Abbeel, and Wojciech Zaremba. Hindsight Experience Replay. 2017. doi: 10.48550/ARXIV.1707.01495. URL <https://arxiv.org/abs/1707.01495>.
- Shangdong Zhang and Richard S. Sutton. A Deeper Look at Experience Replay, 2017. URL <https://arxiv.org/abs/1712.01275>.
- David Isele and Akansel Cosgun. Selective Experience Replay for Lifelong Learning. *Proceedings of the AAAI Conference on Artificial Intelligence*, 32(1), April 2018. ISSN 2374-3468, 2159-5399. doi: 10.1609/aaai.v32i1.11595. URL <https://ojs.aaai.org/index.php/AAAI/article/view/11595>.
- David Rolnick, Arun Ahuja, Jonathan Schwarz, Timothy P. Lillicrap, and Greg Wayne. Experience Replay for Continual Learning, 2018. URL <https://arxiv.org/abs/1811.11682>.
- Mohammad Rostami, Soheil Kolouri, and Praveen K. Pilly. Complementary Learning for Overcoming Catastrophic Forgetting Using Experience Replay, 2019. URL <https://arxiv.org/abs/1903.04566>.
- William Fedus, Prajit Ramachandran, Rishabh Agarwal, Yoshua Bengio, Hugo Larochelle, Mark Rowland, and Will Dabney. Revisiting Fundamentals of Experience Replay, 2020. URL <https://arxiv.org/abs/2007.06700>.
- Cong Lu, Philip J. Ball, Yee Whye Teh, and Jack Parker-Holder. Synthetic Experience Replay, 2023. URL <https://arxiv.org/abs/2303.06614>.
- Mirza Ramicic and Andrea Bonarini. Entropy-based prioritized sampling in Deep Q-learning. In *2017 2nd International Conference on Image, Vision and Computing (ICIVC)*, pages 1068–1072, Chengdu, China, June 2017. IEEE. ISBN 9781509062386. doi: 10.1109/ICIVC.2017.7984718. URL <http://ieeexplore.ieee.org/document/7984718/>.
- Jiashan Gao, Xiaohui Li, Weihui Liu, and Jingchao Zhao. Prioritized Experience Replay Method Based on Experience Reward. In *2021 International Conference on Machine Learning and Intelligent Systems Engineering (MLISE)*, pages 214–219, Chongqing, China, July 2021. IEEE. ISBN 9781665417365. doi: 10.1109/MLISE54096.2021.00045. URL <https://ieeexplore.ieee.org/document/9611651/>.
- Su Young Lee, Sungik Choi, and Sae-Young Chung. Sample-Efficient Deep Reinforcement Learning via Episodic Backward Update, 2018. URL <https://arxiv.org/abs/1805.12375>.
- Marc Brittain, Josh Bertram, Xuxi Yang, and Peng Wei. Prioritized Sequence Experience Replay, 2019. URL <https://arxiv.org/abs/1905.12726>.
- Daochen Zha, Kwei-Herng Lai, Kaixiong Zhou, and Xia Hu. Experience Replay Optimization. In *Proceedings of the Twenty-Eighth International Joint Conference on Artificial Intelligence*, pages 4243–4249, Macao, China, August 2019. International Joint Conferences on Artificial Intelligence Organization. ISBN 9780999241141. doi: 10.24963/ijcai.2019/589. URL <https://www.ijcai.org/proceedings/2019/589>.
- Youngmin Oh, Kimin Lee, Jinwoo Shin, Eunho Yang, and Sung Ju Hwang. Learning to Sample with Local and Global Contexts in Experience Replay Buffer, April 2021. URL <http://arxiv.org/abs/2007.07358>. arXiv:2007.07358 [cs, stat].
- Matthew Aitchison, Penny Sweetser, and Marcus Hutter. Atari-5: Distilling the Arcade Learning Environment down to Five Games, 2022. URL <https://arxiv.org/abs/2210.02019>.
- R.S. Sutton and A.G. Barto. Reinforcement Learning: An Introduction. *IEEE Transactions on Neural Networks*, 9(5):1054–1054, September 1998. ISSN 1045-9227, 1941-0093. doi: 10.1109/TNN.1998.712192. URL <https://ieeexplore.ieee.org/document/712192/>.
- Christopher Watkins. *Learning From Delayed Rewards*. PhD thesis, Kings College, London, 1989.
- Christopher J. C. H. Watkins and Peter Dayan. Q-learning. *Machine Learning*, 8(3-4):279–292, May 1992. ISSN 0885-6125, 1573-0565. doi: 10.1007/BF00992698. URL <http://link.springer.com/10.1007/BF00992698>.
- A Rupam Mahmood, Hado P van Hasselt, and Richard S. Sutton. Off-policy learning based on weighted importance sampling with linear computational complexity. *Advances in Neural Information Processing Systems*, pages 3014–3022, 2014.

- Mark Towers, Ariel Kwiatkowski, Jordan Terry, John U. Balis, Gianluca De Cola, Tristan Deleu, Manuel Goulão, Andreas Kallinteris, Markus Krimmel, Arjun KG, Rodrigo Perez-Vicente, Andrea Pierré, Sander Schulhoff, Jun Jet Tai, Hannah Tan, and Omar G. Younis. Gymnasium: A Standard Interface for Reinforcement Learning Environments, 2024. URL <https://arxiv.org/abs/2407.17032>.
- John W. Tukey. *Exploratory Data Analysis*. Addison-Wesley Publishing Company, Reading, Mass, 1977. URL <https://www.science.org/doi/10.1126/science.200.4338.195.a>.
- Hado van Hasselt, Arthur Guez, and David Silver. Deep Reinforcement Learning with Double Q-learning, 2015. URL <https://arxiv.org/abs/1509.06461>.
- Antonin Raffin. RL baselines3 zoo. <https://github.com/DLR-RM/rl-baselines3-zoo>, 2020.
- Volodymyr Mnih, Koray Kavukcuoglu, David Silver, Andrei A. Rusu, Joel Veness, Marc G. Bellemare, Alex Graves, Martin Riedmiller, Andreas K. Fidjeland, Georg Ostrovski, Stig Petersen, Charles Beattie, Amir Sadik, Ioannis Antonoglou, Helen King, Dhharshan Kumaran, Daan Wierstra, Shane Legg, and Demis Hassabis. Human-level control through deep reinforcement learning. *Nature*, 518(7540):529–533, February 2015. ISSN 0028-0836, 1476-4687. doi: 10.1038/nature14236. URL <https://www.nature.com/articles/nature14236>.
- Antonin Raffin, Quentin Gallouédec, Noah Dormann, Adam Gleave, Anssi, Alex Pasquali, Juan Rocamonde, M. Ernestus, Patrick Helm, Thomas Simonini, Quinn Sinclair, Corentin, Rohan Tangri, Sidney Tio, Tobias Rohrer, Tom Dörr, Wilson, Steven H. Wang, Sam Toyer, Roland Gavrilescu, Paul Maria Scheikl, Parth Kothari, Oleksii Kachaiev, Megan Klaiiber, Marsel Khisamurdinov, Mark Towers, Jan-Hendrik Ewers, Grégoire Passault, Dominic Kerr, and Costa Huang. Stable-Baselines3 v2.4.0, November 2024. URL <https://zenodo.org/doi/10.5281/zenodo.14178439>.
- Volodymyr Mnih, Koray Kavukcuoglu, David Silver, Alex Graves, Ioannis Antonoglou, Daan Wierstra, and Martin Riedmiller. Playing Atari with Deep Reinforcement Learning, 2013. URL <https://arxiv.org/abs/1312.5602>.
- Abien Fred Agarap. Deep Learning using Rectified Linear Units (ReLU), 2018. URL <https://arxiv.org/abs/1803.08375>.

A Algorithm

Algorithm 2: Deep Q Learning with reliability-adjusted proportional prioritization

Input: batch size k , learning rate η , replay period K , replay buffer size N , exponents α, ω and β , budget T .

```

1 Initialize replay memory  $\mathcal{H} = \emptyset$ ,  $\Delta = 0$ ,  $p_1 = 1$ , episode vector  $\phi = \mathbf{0}^{(N)}$ , episodic count  $\Phi = 1$  and maximum
  sum of episodic TDE  $F = 1$ ;
2 Observe  $S_1$  and choose  $A_1 \sim \pi_\theta(S_1)$ ;
3 for  $c \in \{1, \dots, T\}$  do
4   Initialize accumulated weight change  $\Delta = 0$  and empty batch  $\mathcal{X} = \mathbf{0}^{(k)}$ ;
5   Observe  $S_{c+1}, R_c, d_c$ ;
6   Store transition  $C_c = (S_c, A_c, R_c, d_c, S_{c+1})$  in  $\mathcal{H}$  with  $\phi_c = \Phi$  and  $p_c = \max_t(p_t)$  for all  $t \in \{1, \dots, N\}$ ;
7   if  $c \equiv 0 \pmod K$  then
8     for  $m \in \{1, \dots, k\}$  do
9       Sample a transition  $C_j$  from  $\mathcal{H}$  to add to batch  $\mathcal{X}$  such that  $\mathbb{P}(C_t = \mathcal{X}_m) = p_t$  for all  $t \in \{1, \dots, N\}$ ;
10      Compute importance-sampling weight  $w_j = \frac{(N \cdot p_j)^{-\beta}}{\max_t w_t}$  for all  $t \in \{1, \dots, N\}$ ;
11      Compute TDE  $\delta_j = Q_{target}(S_j) - Q(S_j, A_j)$ ;
12      Accumulate weight-change  $\Delta \leftarrow \Delta + w_j \cdot \delta_j \cdot \nabla_\theta Q(S_j, A_j)$ ;
13    end
14    Update weights  $\theta \leftarrow \theta + \eta \cdot \Delta$ ;
15    From time to time, copy weights into target network,  $\theta_{target} \leftarrow \theta$ ;
16    Update maximum sum of absolute TDEs,  $F \leftarrow \max_{t \in \{1, \dots, N\}} \left( \sum_{i=1}^N \delta_i^+ \cdot \mathbb{1}_{\phi_t = \phi_i} \right)$ ;
17    for  $t \in \{1, \dots, N\}$  do
18      Compute TDE reliabilities,  $\mathcal{R}_t = \begin{cases} 1 - \left( \frac{\sum_{i=t+1}^N \delta_i^+}{\sum_{i=1}^N \delta_i^+} \right) & \text{for transitions of terminated episodes} \\ 1 - \left( \frac{F - \sum_{i=1}^t \delta_i^+}{F} \right) & \text{for transitions of ongoing episodes} \end{cases}$ 
19      Update transition sampling criterion  $\Psi_t \leftarrow \mathcal{R}_t^\omega \cdot \delta_t^{+\alpha}$ ;
20      Update transition priorities  $p_t \leftarrow \frac{\Psi_t}{\sum_{i=1}^N \Psi_i}$ ;
21    end
22  end
23  if  $d_c = 1$  then
24    for  $t \in \{1, \dots, N\} \mid \phi_t = \phi_c$  do
25      Compute TDE reliabilities for the finished episode,  $R_t = 1 - \left( \frac{\sum_{i=t+1}^N \delta_i^+}{\sum_{i=1}^N \delta_i^+} \right)$ ;
26    end
27     $\Phi \leftarrow \Phi + 1$ ;
28  end
29  Choose action  $A_c \sim \pi_\theta(S_c)$ ;
30 end

```

In the following, we describe how ReaPER operates in conjunction with a Deep Q-Network (DQN). The agent begins by observing the initial state and selecting an action (Algorithm 2, Line 2).

For a fixed number of iterations, the agent interacts with the environment, observes the resulting transition from its latest action, and stores this transition in the replay buffer with maximum priority (Algorithm 2, Line 5f.).

Every K steps, the agent performs a training update (Algorithm 2, Line 7). During training, it samples a batch \mathcal{X} from the buffer using the current priorities p as sampling weights (Algorithm 2, Line 8ff.). The agent updates the model parameters using importance-sampling-weighted TD-errors (Algorithm 2, Line 14), and uses the observed TD-errors to update the priorities p for all transitions in the batch (Algorithm 2, Line 17ff.). This involves recomputing the reliabilities based on the new TD-errors, applying a conservative estimate for transitions from ongoing episodes (Algorithm 2, Line 18). The agent then recalculates the sampling criterion Φ and updates the priorities p accordingly (Algorithm 2, Line 20), concluding the training step.

Upon episode termination, the agent replaces the preliminary reliability estimate with the actual reliability (Algorithm 2, Line 25). Throughout training, it tracks episode progress to enable continuous recomputation of reliabilities (Algorithm 2, Line 27).

At each iteration, the agent selects the next action based on its current policy and state (Algorithm 2, Line 29), initiating the next cycle.

B Detailed formal analysis

We subsequently theoretically explore the properties of ReaPER. This section extends the formal analysis in Section 3.2.

B.1 Convergence behavior

In the following, we provide a formal motivation for ReaPER by analyzing the influence of target bias on convergence behavior. We do so by showing that a misaligned target may degrade the value function, and then provide a decomposition of the expected error update.

Lemma B.1 (Update misalignment due to target bias). *Let $\mathbf{g}_t = \nabla_\theta(Q(S_t, A_t) - Q_{\text{target}}(S_t))^2$ denote the gradient of the TDE loss and let $\mathbf{g}_t^* = \nabla_\theta(Q(S_t, A_t) - Q^*(S_t, A_t))^2$ be the ideal gradient that aligns with the true value error. Then,*

$$\langle \mathbf{g}_t, \mathbf{g}_t^* \rangle = 2(Q(S_t, A_t) - Q^*(S_t, A_t))^2 - 2(Q(S_t, A_t) - Q^*(S_t, A_t))\varepsilon_t. \quad (19)$$

Proof of Lemma B.1. We compute the gradients explicitly. We define

$$e_t := Q(S_t, A_t) - Q^*(S_t, A_t), \quad \varepsilon_t := Q_{\text{target}}(S_t) - Q^*(S_t, A_t). \quad (20)$$

We now may rewrite the TDE,

$$\delta_t = Q_{\text{target}}(S_t) - Q(S_t, A_t) = (Q^*(S_t, A_t) + \varepsilon_t) - Q(S_t, A_t) = -e_t + \varepsilon_t. \quad (21)$$

Now, the gradients are

$$\mathbf{g}_t = 2(Q(S_t, A_t) - Q_{\text{target}}(S_t))\nabla_\theta Q = 2(-\delta_t)\nabla_\theta Q(S_t, A_t), \quad (22)$$

$$\mathbf{g}_t^* = 2(Q(S_t, A_t) - Q^*(S_t, A_t))\nabla_\theta Q(S_t, A_t) = 2e_t\nabla_\theta Q(S_t, A_t). \quad (23)$$

Hence,

$$\langle \mathbf{g}_t, \mathbf{g}_t^* \rangle = 4(-\delta_t)e_t\|\nabla_\theta Q(S_t, A_t)\|^2 = 4(e_t - \varepsilon_t)e_t\|\nabla_\theta Q(S_t, A_t)\|^2. \quad (24)$$

Simplifying yields

$$\langle \mathbf{g}_t, \mathbf{g}_t^* \rangle = 4(e_t^2 - e_t\varepsilon_t)\|\nabla_\theta Q(S_t, A_t)\|^2, \quad (25)$$

which proves the result up to a constant factor of the norm. \square

This result shows that even when the TDE is large, its usefulness critically depends on the reliability of the target value. When ε_t is large, the update may not improve the value function estimation. When ε_t is sign-misaligned with the current true estimation error e_t , the update will even degrade the value function, pushing $Q(S_t, A_t)$ further away from $Q^*(S_t, A_t)$.

Based on these considerations, we proceed to compare various sampling strategies by analyzing the expected change in the squared Q-value error caused by a single update step. The following lemma provides a decomposition of this change and builds the foundation of our main theoretical result.

Lemma B.2 (Expected error update under sampling strategy μ). *Let $e_t = (Q(S_t, A_t) - Q^*(S_t, A_t))$. Let Q denote the Q-function before an update, and let Q' denote the Q-function after the update. Let $\mathbb{E}_\mu[\Delta\|Q(S_t, A_t) - Q^*(S_t, A_t)\|^2] = \mathbb{E}_\mu[\|Q'(S_t, A_t) - Q^*(S_t, A_t)\|^2 - \|Q(S_t, A_t) - Q^*(S_t, A_t)\|^2]$. Then,*

$$\begin{aligned} \mathbb{E}_\mu[\Delta\|Q(S_t, A_t) - Q^*(S_t, A_t)\|^2] &= 2\eta \sum_{t=1}^n \mu_t \mathbb{E}[(Q(S_t, A_t) - Q^*(S_t, A_t))\varepsilon_t] \\ &\quad + \eta^2 \sum_{t=1}^n \mu_t \mathbb{E}[\delta_t^2] - 2\eta \sum_{t=1}^n \mu_t \mathbb{E}[e_t^2]. \end{aligned} \quad (26)$$

Proof of Lemma B.2. We analyze the Q-value update

$$Q'(S_t, A_t) = Q(S_t, A_t) + \eta \delta_t. \quad (27)$$

After the update

$$Q'(S_t, A_t) - Q^*(S_t, A_t) = Q(S_t, A_t) + \eta \delta_t - Q^*(S_t, A_t) = e_t + \eta \delta_t, \quad (28)$$

the squared error becomes

$$(Q'(S_t, A_t) - Q^*(S_t, A_t))^2 = (e_t + \eta \delta_t)^2 = e_t^2 + 2\eta e_t \delta_t + \eta^2 \delta_t^2. \quad (29)$$

The expectation under sampling distribution μ is

$$\mathbb{E}[\Delta e_t] = \eta^2 \mathbb{E}[\delta_t^2] + 2\eta \mathbb{E}[e_t \delta_t]. \quad (30)$$

Note that $\delta_t = Q_{\text{target}}(S_t) - Q(S_t, A_t) = \varepsilon_t - e_t$, so

$$e_t \delta_t = e_t(\varepsilon_t - e_t) = e_t \varepsilon_t - e_t^2, \quad (31)$$

hence

$$\mathbb{E}[\Delta e_t] = \underbrace{\eta^2 \mathbb{E}[\delta_t^2]}_{(1)} - \underbrace{\mathbb{E}[e_t^2]}_{(2)} + \underbrace{2\eta \mathbb{E}[e_t \varepsilon_t]}_{(3)}. \quad (32)$$

Summing over all transitions with μ_t gives the result. \square

This decomposition highlights three components: (1) the variance of the TDE, (2) the true squared error and (3) the bias-error-interaction. The latter is key to explaining why ReaPER outperforms other sampling strategies.

A key factor in the reliability of bootstrapped targets is the extent of downstream TDEs. Intuitively, if future states still exhibit significant TDEs, the bootstrapped target for the current state is more likely to be biased. This motivates the following technical assumption.

B.2 Discussion of Assumption 3.4

Assumption 3.4 establishes a relationship between the target bias for a given transition and the sum of TDEs for downstream transitions. This aligns with a conventional perspective in TD-learning analysis, wherein bootstrapped targets predominantly inherit bias from inaccuracies in future value estimates.

Although Assumption 3.4 appears rather limiting at first sight, it is in fact less strict than assumptions made in classical Q-learning analyses: classical Q-learning convergence proofs (see, e.g., Watkins & Dayan, 1992) rely on global exploration assumptions, ensuring that every state-action pair is visited infinitely often, and on decaying learning rates to control noise. In contrast, Assumption 3.4 takes a more local view, postulating that the target bias along an observed trajectory can be bounded by unresolved downstream TDEs. While classical assumptions ensure eventual global accuracy, our assumption focuses on bounding the bias during finite-sample learning along actual agent trajectories, which is more aligned with practical deep RL settings.

Under Assumption 3.4, the reliability score \mathcal{R}_t — which measures the proportion of downstream TDE along a trajectory — provides an upper bound on the normalized target bias ε_t . Lemma 3.5 formalizes this relationship.

B.3 Proof of Lemma 3.5

Proof. From the definition of \mathcal{R}_t , we have

$$1 - \mathcal{R}_t = \frac{\sum_{i=t+1}^n \delta_i^+}{\sum_{i=1}^n \delta_i^+}. \quad (33)$$

Multiplying both sides by $\sum_{i=1}^n \delta_i^+$, we obtain

$$\sum_{i=t+1}^n \delta_i^+ = (1 - \mathcal{R}_t) \cdot \sum_{i=1}^n \delta_i^+. \quad (34)$$

Substituting this into Assumption 3.4, we find

$$|\varepsilon_t| \leq \lambda \sum_{i=t+1}^n \delta_i^+ = \lambda(1 - \mathcal{R}_t) \cdot \sum_{i=1}^n \delta_i^+, \quad (35)$$

which proves the first inequality.

Rearranging the result gives

$$\mathcal{R}_t \leq 1 - \frac{|\varepsilon_t|}{\lambda \sum_{i=1}^n \delta_i^+}, \quad (36)$$

completing the proof. \square

Moreover, it follows that

$$\mathcal{R}_t \leq 1 - \frac{|\varepsilon_t|}{\lambda \sum_{i=1}^n \delta_i^+}. \quad (37)$$

Lemma 3.5 provides a formal link between the reliability score \mathcal{R}_t used in ReaPER and the target bias ε_t . Under Assumption 3.4, transitions with large downstream TDEs (i.e., large $\sum_{i=t+1}^n \delta_i^+$) likely suffer from higher target bias. This justifies using \mathcal{R}_t to down-weight transitions with unreliable TDEs in the sampling distribution as long as downstream transitions suffer from high TDE. Consequently, ReaPER not only emphasizes transitions with high learning potential (large δ_t^+) but also prioritizes those with more reliable target estimates.

B.4 Proof of Proposition 3.6

Proof. From Lemma B.2, the expected change in squared error per update, conditioned on the current Q-function, is

$$\Delta E = \eta^2 \sum_{t=1}^n \mu_t \mathbb{E}[\delta_t^2] - 2\eta \sum_{t=1}^n \mu_t \mathbb{E}[e_t^2] + 2\eta \sum_{t=1}^n \mu_t \mathbb{E}[e_t \varepsilon_t]. \quad (38)$$

We seek to maximize the second term (true error reduction) while minimizing the third term (bias-error-interaction). The analysis proceeds by comparing the terms under the different sampling strategies.

We now compare three sampling strategies:

Uniform sampling ($\mu_t = 1/n$): No prioritization occurs. Transitions with small e_t^2 and potentially large $e_t \varepsilon_t$ are sampled proportionally to their frequency of occurrence in the buffer. Hence, both the error reduction term $\sum_t \mu_t \mathbb{E}[e_t^2]$ and the bias term $\sum_t \mu_t \mathbb{E}[e_t \varepsilon_t]$ are solely determined by the buffer content, and sampling does not reduce error or bias.

PER sampling ($\mu_t \propto (\delta_t^+)$): PER prioritizes transitions with large TDE δ_t^+ , which correlates with larger e_t^2 . As such, the sampling increases error reduction over buffer content,

$$\sum_{t=1}^n \mu_t^{\text{PER}} \mathbb{E}[e_t^2] \gg \sum_{t=1}^n \mu_t^{\text{Uniform}} \mathbb{E}[e_t^2], \quad (39)$$

leading to faster true error reduction compared to uniform sampling. However, PER does not account for target bias ε_t . Nevertheless, since PER focuses updates on transitions with large TDEs (rather than arbitrary ones), it slightly reduces the bias-error-interaction compared to uniform:

$$\sum_{t=1}^n \mu_t^{\text{PER}} \mathbb{E}[e_t \varepsilon_t] \ll \sum_{t=1}^n \mu_t^{\text{Uniform}} \mathbb{E}[e_t \varepsilon_t]. \quad (40)$$

ReaPER sampling ($\mu_t \propto \mathcal{R}_t \delta_t^+$): Prioritizes transitions with large TDE *and* high reliability \mathcal{R}_t , thus additionally considering target bias (see Lemma B.3). Thus, ReaPER achieves

$$\sum_{t=1}^n \mu_t^{\text{ReaPER}} \mathbb{E}[e_t^2] \gg \sum_{t=1}^n \mu_t^{\text{PER}} \mathbb{E}[e_t^2] \gg \sum_{t=1}^n \mu_t^{\text{Uniform}} \mathbb{E}[e_t^2], \quad (41)$$

for the true error term, and

$$\sum_{t=1}^n \mu_t^{\text{ReaPER}} \mathbb{E}[e_t \varepsilon_t] \ll \sum_{t=1}^n \mu_t^{\text{PER}} \mathbb{E}[e_t \varepsilon_t] \ll \sum_{t=1}^n \mu_t^{\text{Uniform}} \mathbb{E}[e_t \varepsilon_t], \quad (42)$$

for the bias term.

Therefore, ReaPER leads to the steepest expected decrease in squared error per update, followed by PER, followed by uniform sampling. Summing the per-step improvements over training steps, we conclude

$$\mathbb{E}_{\mu^{\text{Uniform}}} [\|Q_T - Q^*\|^2] \geq \mathbb{E}_{\mu^{\text{PER}}} [\|Q_T - Q^*\|^2] \geq \mathbb{E}_{\mu^{\text{ReaPER}}} [\|Q_T - Q^*\|^2], \quad (43)$$

as claimed. \square

B.5 Discussion of Remark 3.7

While Assumption 3.4 is stated under the premise that the agent follows an optimal policy, it can be extended to fixed but suboptimal policies. We now briefly outline the modifications necessary if the agent follows a fixed but suboptimal policy. In this case, the target bias ε_t cannot be bounded solely by unresolved downstream TDEs, as suboptimal actions introduce an additional, trajectory-independent bias. Formally, suppose there exists a constant $\zeta \geq 0$ such that for all transitions along observed trajectories,

$$|Q^\pi(S_t, A_t) - Q^*(S_t, A_t)| \leq \zeta, \quad (44)$$

where Q^π denotes the action-value function under the fixed policy π . Then, under analogous reasoning to Assumption 3.4, the target bias satisfies

$$|\varepsilon_t| \leq \lambda \sum_{i=t+1}^n \delta_i^+ + \zeta. \quad (45)$$

This adjusted bound propagates through the subsequent results. In particular, Lemma B.3 becomes

$$|\varepsilon_t| \leq \lambda(1 - \mathcal{R}_t) \sum_{i=1}^n \delta_i^+ + \zeta, \quad (46)$$

and the reliability bound adjusts accordingly. In the error decomposition of Lemma B.2 and the convergence hierarchy in Proposition B.4, the additive term ζ introduces a bias floor that does not vanish through learning. Consequently, while ReaPER still achieves improved sampling efficiency by reducing the impact of target misalignment, the achievable Q-function accuracy is ultimately lower-bounded by ζ . In the limit as $\zeta \rightarrow 0$ (the policy approaches optimality), we recover the original theory.

B.6 Proof of Proposition 3.8

Proof. First, we note that we can assume without loss of generality that there is a $\tau > 0$ such that the distribution μ^* satisfies

$$\sum_{i=1}^N \mu_i^* \delta_i^+ \geq \tau. \quad (47)$$

If such a $\tau > 0$ does not exist, that implies $\sum_{i=1}^N \mu_i^* \delta_i^+$ which only holds if $\delta_i = 0$ for all $i = 1, \dots, N$ — a setting in which any sampling distribution from the buffer is optimal. Hence, equipped with (47), the optimal sampling distribution μ^* is characterized as a solution to the following optimization problem

$$\min_{\mu \in \Delta_N} \sum_{i=1}^N \mu_i \sigma_i^2 \quad (48)$$

$$\text{subject to } \sum_{i=1}^N \mu_i \delta_i^+ \geq \tau. \quad (49)$$

We introduce Lagrange multipliers $\lambda \geq 0$ for the inequality constraint and ν for the probability normalization constraint. Then, the Lagrangian reads

$$\mathcal{L}(\mu, \lambda, \nu) = \sum_{i=1}^N \mu_i \sigma_i^2 + \lambda \left(\tau - \sum_{i=1}^N \mu_i \delta_i^+ \right) + \nu \left(1 - \sum_{i=1}^N \mu_i \right) \quad (50)$$

The KKT conditions for optimality are:

$$\text{(Stationarity)} \quad \frac{\partial \mathcal{L}}{\partial \mu_i} = \sigma_i^2 - \lambda \delta_i^+ - \nu = 0 \quad \text{for all } i = 1, \dots, N \quad (51)$$

$$\text{(Primal feasibility)} \quad \sum_{i=1}^N \mu_i \delta_i^+ \geq \tau, \quad \sum_{i=1}^N \mu_i = 1, \quad \mu_i \geq 0 \quad (52)$$

$$\text{(Dual feasibility)} \quad \lambda \geq 0 \quad (53)$$

$$\text{(Complementary slackness)} \quad \lambda \left(\tau - \sum_{i=1}^N \mu_i \delta_i^+ \right) = 0 \quad (54)$$

In the following we distinguish two cases.

Case 1: Suppose $\sum_{i=1}^N \mu_i \delta_i^+ > \tau$. Then, complementary slackness implies $\lambda = 0$. The stationarity condition becomes

$$\sigma_i^2 - \nu = 0 \quad \Rightarrow \quad \sigma_i^2 = \nu \quad \text{for all } i = 1, \dots, N, \quad (55)$$

which is only possible if all σ_i^2 are equal. In general, this is not the case, so the constraint must be active at optimality.

Case 2: Then $\sum_{i=1}^N \mu_i \delta_i^+ = \tau$, and complementary slackness implies $\lambda > 0$. From the stationarity condition, we obtain

$$\sigma_i^2 - \lambda \delta_i^+ - \nu = 0 \quad \Rightarrow \quad \sigma_i^2 = \lambda \delta_i^+ + \nu \quad (56)$$

Solving for λ , we get

$$\lambda = \frac{\sigma_i^2 - \nu}{\delta_i^+} \quad (57)$$

This must hold for all $i = 1, \dots, N$, so the right-hand side must be constant across i , which implies

$$\frac{\sigma_i^2}{\delta_i^+} - \frac{\nu}{\delta_i^+} = \text{constant} \quad \xRightarrow{(a)} \quad \mu_i^* \propto \frac{\delta_i^+}{\sigma_i^2} \quad (58)$$

To justify the implication (a), note that the stationarity condition directly states $\sigma_i^2 - \nu = \lambda \delta_i^+ \Rightarrow \frac{1}{\lambda} = \frac{\delta_i^+}{\sigma_i^2 - \nu}$. Therefore, a higher value $\frac{\delta_i^+}{\sigma_i^2 - \nu}$ implies a higher gradient contribution exactly where μ_i should be large. \square

C Results in a stylized setting

We consider a single episode within a stylized setting. The agent is following the optimal path, $Q_{\text{target}}(S_t) = Q(S_{t+1}, A_{t+1})$ where $A_{t+1} = \pi^*(S_{t+1})$ for all $t \in \{1, \dots, n-1\}$. At the end of this episode, the agent obtains a final reward $R_n = 1$. There are no intermediary rewards. The agent aims to learn the correct Q-values for all transitions within this trial using a Tabular Q-learning (TQL) approach (Watkins and Dayan [1992]). $Q_{\text{target}}(S_t)$ are continuously updated to be $Q(S_{t+1}, A_{t+1})$, with $Q_{\text{target}}(S_n)$ being 1. We consider a transition C_t to be learned if the Q-value reaches its (for real applications mostly unknown) ground-truth Q-value, $Q(S_t, A_t) = Q^*(S_t, A_t)$. We consider the model to have converged when all Q-values reach their ground-truth Q-value, $Q(S_t, A_t) = Q^*(S_t, A_t)$ for $t \in \{1, \dots, n\}$. This is the case when all TDEs within this trial have a value of 0, i.e., $\delta_t = 0$ for $t \in \{1, \dots, n\}$.

The agent learns by repeatedly selecting k transition indices. For every selected transition C_j , the Bellman equation is solved to update the Q-value, $Q(S_j, A_j) \leftarrow Q(S_j, A_j) + \gamma \cdot \delta_j$. For the sake of simplicity, we assume a discount factor $\gamma = 1$, a batch size $k = 1$, and a learning rate $\eta = 1$. As $\eta = 1$, learning on a transition C_j implies setting the Q-value to Q_{target} , i.e., $Q(S_j, A_j) = Q_{\text{target}}(S_j)$. We repeat this iterative process of sampling and the respective Q-value adaptation until the model converged.

We use three different selection strategies to identify the transition index j , which determines the transition C_j that the model trains on next, uniform sampling, Greedy Prioritized Experience Replay (PER-g), and Greedy Reliability-adjusted Prioritized Experience Replay (ReaPER-g). Uniform sampling selects transitions at random with equal probability. PER-g selects the transition with the highest TDE δ . ReaPER-g selects the transition with the highest reliability-adjusted TDE Ψ . In both PER-g and ReaPER-g, if there is no unique maximum, ties are resolved by random choice.

We compare these selection strategies to the optimal solution, the *Oracle*. The Oracle selects the transition C_l with the highest index that has a absolute TDE greater than zero, $l = \max(t \mid \delta_t \neq 0)$ for $t \in \{1, \dots, n\}$. Given $\eta = 1$, using the Oracle, the agent will always converge within $\sum_{t=1}^n \mathbb{1}_{\delta_t \neq 0} \leq n$ steps and is therefore optimal. We compare the sampling strategies under varying levels of Q_{target} reliability. Q_{target} reliability here is determined by the extent of target Q-values for unlearned transitions without immediate reward varying from zero: Reliability is high if Q_{target} values remains close to the immediate observed reward unless specifically learned otherwise. Q_{target} reliability decreases with more Q_{target} values deviating from zero without observation of an immediate reward and without being explicitly learned. In reality, this may happen either through Q-value initialization or - more importantly, when using Q-functions - erroneous Q-value generalization across state-action pairs.

In the present example, we simulate different levels of Q_{target} reliability using different Q-value initializations. Specifically, we consider three Q_{target} reliability conditions: High, medium and low Q_{target} reliability. In all conditions, all $Q(S_t, A_t)$ for $t \in \{1, \dots, n\}$ are first initialized to zero. Then, depending on the reliability condition, some of these initializations are overwritten with ones to induce unreliability. In the *low reliability* condition, every second Q-value is overwritten. In the *medium reliability* condition, every fourth Q-value is overwritten. In the *high reliability* condition, no value is overwritten.

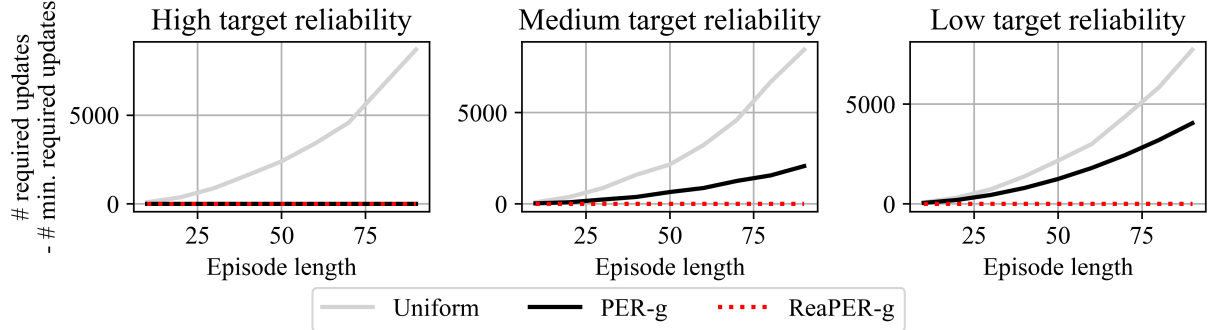


Figure 4: Performance comparison in a stylized setting for three sampling methods; uniform sampling, PER-g, and ReaPER-g. Performance is quantified as the number of updates until convergence minus the minimally required number of updates given by an Oracle. Each sampling method is evaluated using different episode lengths (between 10 and 100) and different levels of Q_{target} reliability (high, medium and low).

We employ every selection mechanism to train until convergence for episodes of length 10 to 100 across all reliability conditions. As shown in Figure 2, uniform sampling converges the slowest across all reliability conditions. PER-g finds the optimal transition selection order when target reliability is high. However, PER-g’s convergence speed quickly diminishes as Q_{value} reliability decreases. ReaPER-g on the other hand actively accounts for changes in Q_{value} reliability. By doing so, it consistently finds the ideal solution regardless of Q_{value} reliability.

D Experimental settings

All training parameters for all environments were set to according to pre-existing recommendations from previous research Schaul et al. [2015], van Hasselt et al. [2015], Raffin [2020]. The full experimental settings are subsequently described in detail to enable full reproducibility.

Experience replay parameters Following the suggestion for proportional PER for DDQN in Schaul et al. [2015], α was set to 0.6 for PER. As we expect increased need for regularization due to the reliability-driven priority scale-down, we expected values smaller values for α and ω in ReaPER. We performed minimal hyperparameter tuning to find a suitable configuration. We did so by training a single game, QBERT, on three configurations for α and ω , (1) $\alpha = 0.2$, $\omega = 0.4$, (2) $\alpha = 0.3$, $\omega = 0.3$ and (3) $\alpha = 0.4$, $\omega = 0.2$. For the runs presented in the paper, the best-performing variant ($\alpha = 0.4$, $\omega = 0.2$) was used. For both PER and ReaPER, β linearly increased with training time, $\beta \leftarrow (0.4 \rightarrow 1.0)$ as proposed in Schaul et al. [2015]. A buffer size of 10^6 was used.

Atari preprocessing As in Mnih et al. [2015], Atari frames were slightly modified before being processed by the network. Preprocessing was performed using StableBaselines3’s *AtariWrapper* (Antonin Raffin et al. [2024]). All image inputs were rescaled to an 84x84 grayscale image. After resetting the environment, episodes were started with a randomized number of *NoOp*-frames (up to 30) without any operation by the agent, effectively randomizing the initial state and consequently preventing the agent from learning a single optimal path through the game. Four consecutive frames were stacked to a single observation to provide insight into the direction of movement. Additionally, a termination signal is sent when a life is lost. All these preprocessing steps can be considered standard practice for ATARI games (e.g., Mnih et al. [2013, 2015], Schaul et al. [2015]).

Training specifications Hyperparameters for learning to play CARTPOLE, ACROBOT and LUNARLANDER were set to RL Baselines3 Zoo recommendations (Raffin [2020]). Hyperparameters for learning to play *Atari* games are set based on previous research by Schaul et al. [2015], Mnih et al. [2015] and van Hasselt et al. [2015].

Parameter	CARTPOLE	ACROBOT	LUNARLANDER	ATARI
Learning rate	2.3e-3	6.3e-4	6.3e-4	625e-7
Budget	5e4	1e5	1e5	5e7
Buffer size	1e5	5e4	5e4	1e6
Timestep to start learning	1e3	1e3	1e3	5e4
Target network update interval	10	250	250	3e4
Batch size	64	128	128	32
Steps per model update	256	4	4	4
Number of gradient steps	128	4	4	1
Exploration fraction	0.16	0.12	0.12	0.02
Initial exploration rate	1	1	1	1
Final exploration rate	0.04	0.1	0.1	0.01
Evaluation exploration fraction	0.001	0.001	0.001	0.001
Number of evaluations	100	100	100	200
Trajectories per evaluation	5	5	5	1
Gamma	0.99	0.99	0.99	0.99
Max. gradient norm	10	10	10	∞
Reward threshold	475	-100	200	∞
Optimizer	Adam	Adam	Adam	RMSprop

Network architecture For CARTPOLE, ACROBOT and LUNARLANDER, the network architecture was equivalent to *StableBaselines3*’ default architecture (Antonin Raffin et al. [2024]): A two-layered fully-connected net with 64 nodes per layer was used. For image observations as in the ATARI-5 benchmark, the input was preprocessed to size $84 \times 84 \times 4$. It was then passed through three convolutional layers and two subsequent fully connected layers. The network architecture was equal to the network architecture used in Mnih et al. [2015]. Rectified Linear Units (Agarap [2018]) were used as the activation function.

Evaluation For the environments CARTPOLE, ACROBOT and LUNARLANDER, 100 evaluations were evenly spaced throughout the training procedure. Each agent evaluation consisted of five full trajectories in the environment, going from initial to terminal state. The evaluation score of a single agent evaluation is the average total score across those five evaluation trajectories. Training was stopped when the agent reached a predefined reward threshold defined in the Gymnasium package Towers et al. [2024]. For ATARI environments, as in Schaul et al. [2015], 200 evaluations consisting of a single trajectory were evenly spaced throughout the training procedure. No reward threshold was set.

Score normalization: For ATARI games, scores were normalized to allow for comparability between games. Let Ξ_{raw} denote a single evaluation score that is to be normalized. Let Ξ_{random} denote the score achieved by a randomly initialized policy in this game. Let Ξ_{max} denote the highest score achieved in this game across either condition, ReaPER or PER. The normalized score Ξ_{norm} is then calculated via

$$\Xi_{norm} = \frac{\Xi_{raw} - \Xi_{random}}{\Xi_{high} - \Xi_{random}}. \quad (59)$$

E Atari-5 results

Figure 5 displays the cumulative maximum scores gathered across 200 evaluation periods, which were evenly spaced-out throughout the training runs. ReaPER achieves a higher peak score in BATTLEZONE, NAMETHISGAME, QBERT and PHOENIX. It ties with PER in DOUBLEBUNK.

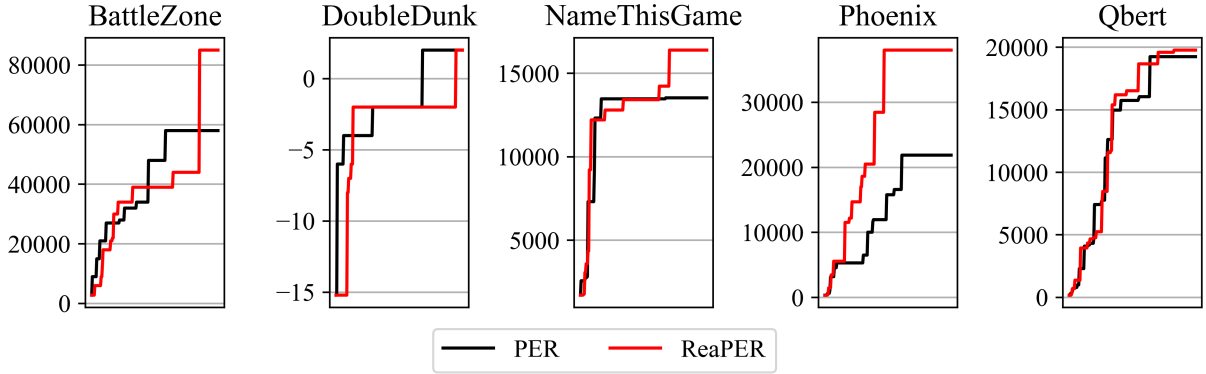


Figure 5: Cumulative maximum evaluation score per game from the ATARI-5 benchmark across the training period

Figure 6 displays the evaluation scores gathered across 200 evaluation periods, which were evenly spaced-out throughout the training runs.

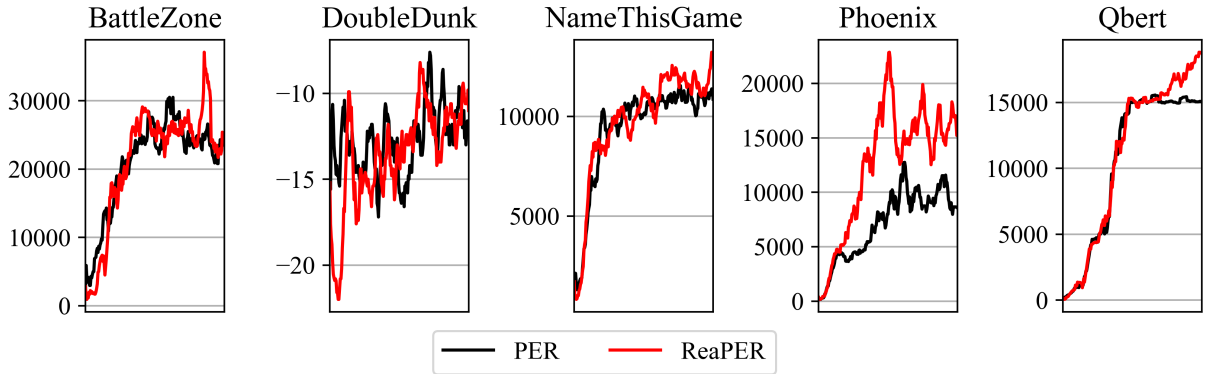


Figure 6: Evaluation scores per game from the ATARI-5 benchmark across the training period with a moving average smoothed over 10 points.

F Hardware specification

The ATARI-5 experiments were conducted on a workstation equipped with an AMD Ryzen 9 7950X CPU (32 cores at 4.5 GHz), 128 GB of RAM, and an NVIDIA RTX 4090 GPU with 24 GB of memory (driver version 12.3). All other numerical experiments were performed on a 2024 MacBook Air with an Apple M3 processor.